Astron. Astrophys. 356, 1023–1030 (2000)

ASTRONOMY AND ASTROPHYSICS

Large scale structures and synchrotron emission

I. Asymmetric supernova remnants

L. Zaninetti[1]

Dipartimento di Fisica Generale, Via Pietro Giuria 1 10125 Torino, Italy (zaninetti@to.infn.it)

Received 8 July 1997 / Accepted 10 February 2000

Abstract. In order to attack the problem of asymmetric shapes of the observed Supernova Remnants, a numerical technique is developed that divides the sphere into many sectors. Using this numerical method, some of the observed features of the supernova remnants, like a barrel shape or multi-ring shape can be reproduced.

Key words: ISM: bubbles – ISM: supernova remnants – radio continuum: stars

1. Introduction

The explosion of a SN should generate circular (spherical in 3D) supernova remnants (hereafter SNR). Conversely, departures from sphericity seem to represent the norm rather than the rule (Gaensler 1998).

By using the fundamental assumption of a symmetric explosion at the beginning, we will try to answer the following questions:

- How does the shape of an explosion evolve in a standard ISM?
- Could characteristic shapes such as a barrel, an ellipse, an egg or a double ring be produced?

In order to answer these questions,a sector approximation has been developed in Sect. 2 that permits the explosion to be followed. In Sect. 3, different types of ISM are analysed and in Sect. 4, the method is applied to SN1006.

2. The 1D radial approximation

The momentum conservation is applied to a conical section with a solid angle $\Delta\ \Omega$, in polar coordinates (McCray 1987)

$$\frac{\mathrm{d}}{\mathrm{dt}}(\Delta \mathrm{MR}) = \Delta \mathrm{F}\,, \tag{1}$$

where

$$\Delta \mathrm{M} = \int_0^{\mathrm{R}} \rho(\mathrm{R},\theta,\phi)\mathrm{dV}\,, \tag{2}$$

Send offprint requests to: L. Zaninetti

is the mass of swept-up interstellar medium in the solid angle $\Delta\ \Omega$, ρ the density of the medium and the driving force:

$$\Delta\ \mathrm{F} = \mathrm{PR}^2\Delta\Omega\,. \tag{3}$$

Here *R*, θ, ϕ are the spherical coordinates; R is the radius, θ the polar angle measured from the vertical axis Z, which in this case is perpendicular to the plane of the galaxy and ϕ the azimuthal angle in the X-Y plane. X,Y and Z are the Cartesian coordinates of the explosion that starts at X=0,Y=0 and Z=0; P represents the pressure as defined in Eq. (5).

Integrating Eq. (1) we obtain:

$$\Delta \mathrm{M}\dot{\mathrm{R}} = \mathrm{PR}^2\mathrm{t} \quad . \tag{4}$$

We now substitute

$$\mathrm{P} = \frac{\frac{2}{3}\mathrm{E}_0}{\Delta \mathrm{V}} \quad , \tag{5}$$

where $\Delta \mathrm{V}$ is the volume occupied by the sphere (uniform medium) or by the ellipsoid (non uniform medium) and E_0 the kinetic energy of the explosion. We now have the following basic differential equation:

$$\dot{\mathrm{R}} = \frac{\frac{2}{3}\mathrm{E}_0\mathrm{R}^2}{\Delta \mathrm{V}\Delta \mathrm{M}}\mathrm{t}\,. \tag{6}$$

2.1. The sector approximation

The differential equation needs to be solved by sectors, with each sector being treated as independent from the others. The rules to increase the radius are based on the swept-up mass in that particular direction, and on the global volume of the explosion.

From a practical point of view, the range of the polar angle θ (180°) will be divided into n_θ steps and the range of the azimuthal angle ϕ (360°) into n_ϕ steps.

This will yield (n_θ +1) (n_ϕ +1) directions of motion that can also be identified with the number of vertices of the polyhedron representing the volume occupied by the explosion; this polyhedron varies from a sphere to an irregular shape on the basis of the swept-up material in each direction. In the plots showing the expansion surface of the explosion, the number of vertices (n_θ+1)·(n_ϕ +1) and the number of the faces $\mathrm{n}_\theta \cdot\ \mathrm{n}_\phi$; are specified, for example in Fig. 7 n_θ=50 and n_ϕ=50.

2.2. The numerical integration

The number of the considered directions is n (the number of vertices). Accordingly, there will be n first order differential equations in one variable involving n functions R_i, $i = 1 \cdots, n$ and the related initial values.

$$\begin{cases} \dot{\mathrm{R}} = \mathrm{f}(\mathrm{t}, \mathrm{R}) \text{ for t } \in [\mathrm{t}_0, \mathrm{t}_{\mathrm{final}}] \text{ where} \\ \mathrm{R}(\mathrm{t}_0) = \mathrm{R}_0 \\ \dot{\mathrm{R}}(\mathrm{t}_0) = \dot{\mathrm{R}}_0 \end{cases} \tag{7}$$

with

$$\mathrm{R} = \begin{bmatrix} \mathrm{R}_1(\mathrm{t}) \\ \vdots \\ \mathrm{R}_\mathrm{n}(\mathrm{t}) \end{bmatrix} \text{ and } \quad \mathrm{f} = \begin{bmatrix} \mathrm{f}_1(\mathrm{t}, \mathrm{R}_1, \ldots, \mathrm{R}_\mathrm{n}) \\ \vdots \\ \mathrm{f}_\mathrm{n}(\mathrm{t}, \mathrm{R}_1, \ldots, \mathrm{R}_\mathrm{n}) \end{bmatrix} \quad . \tag{8}$$

The definitions of R_0, t_0 and $\mathrm{t}_{\mathrm{final}}$ are given in Sect. 2.3. The function f(t,*R*) (the first derivative of the radius), is that of Eq. (6) in each different direction.

The interval $\mathrm{I} = [\mathrm{t}_0, \mathrm{t}_{\mathrm{final}}]$ is called the interval of integration for the differential equation. At each time step $\Delta\mathrm{t}$ the volume of each sector is computed and these n volumes are added together in order to obtain the volumes of the expanding shell. In other words, in the presence of asymmetries, the volume swept up from the explosion is no longer a sphere but could become an egg or an hour-glass. The integrating scheme used is a Runge-Kutta method, and in particular the subroutine RK4 (Press et al. 1992). The integration time $\mathrm{t}_{\mathrm{final}}$ and the time steps Δ t are indicated in the plots.

2.3. The numerical analysis

The first phase of a supernova is the phase with constant velocity $\dot{\mathrm{R}}_0 \approx 10^4$ km/sec; this phase ends at t_0,R_0 (according to McCray 1987; Chevalier 1982; Dickel et al. 1992) when the swept up material equals the ejected material M_{ej}; the point blast stage begins when we reach 8 $\mathrm{M}_\odot$ of swept material. We therefore indicate two times and radii of transition using the symbol $\Leftrightarrow$ (minimum and maximum):

$$\mathrm{t}_0 \approx (0.02 \Leftrightarrow 0.04)(\mathrm{M}_{\mathrm{ej}}/\mathrm{M}_\odot)^{1/3}\mathrm{n}_0^{-1/3}10^4\mathrm{years} \quad , \tag{9}$$

and

$$\mathrm{R}_0 \approx (2 \Leftrightarrow 4)(\mathrm{M}_{\mathrm{ej}}/\mathrm{M}_\odot)^{1/3}\mathrm{n}_0^{-1/3}\mathrm{pc} \quad . \tag{10}$$

At the surface of impact a shock propagates inward into the expanding ejecta, see Chevalier (1982), and another shock propagates outward into the interstellar gas. After a few times t_0 the ejecta have slowed down and transferred most of their kinetic energy into the energy of the outgoing shock.

The presence of anomalies in the ISM could also produce departures from the spherical shape in the so called first phase and therefore the previous initial conditions have been slightly modified on the basis of the first time step Δ t of the numerical code:

$$\mathrm{t}_0 = \Delta\mathrm{t}(10^4\mathrm{years}) \quad , \tag{11}$$

and

$$\mathrm{R}_0 = \dot{\mathrm{R}}_0\Delta\mathrm{t}(10^4\mathrm{years})\mathrm{pc} \quad . \tag{12}$$

With these initial conditions, it is possible to treat the expansion in a medium with constant density as well as in a medium with a spatial density gradient. From the previous formulae it is clear that we should explore SNR with lifetime greater than $\approx$ (200 $\Leftrightarrow$ 400) years; for example SN1006 (Sect. 4). In the case of ISM with constant density, the momentum equation can be easily integrated twice (see, for example McCray 1987) and a well known result is obtained:

$$\mathrm{R} = (\frac{\mathrm{E}_{51}\mathrm{t}_4^2}{\mathrm{n}_0})^{1/5}11.2\mathrm{pc} \quad , \tag{13}$$

t_4 is $\mathrm{t}_{\mathrm{final}}$ expressed in units of 10^4 years, E_{51} is the energy expressed in units of 10^{51} ergs and n_0 is the density expressed in $\mathrm{particles\ cm}^{-3}$. In agreement with McCray ρ_0 = n_0 m was taken, where m = 1.4 m_H. On the basis of this analytical result the reliability of our code was tested.

In the following M_{ej} = 1, $\dot{\mathrm{R}}_0$ = 10000 km/sec (the initial velocity) and E_{51}=1.0. The other variable parameters are indicated in the plots.

In the case of an expansion into a medium with constant density, the energy conserving phase ends at a time $\approx$ 3 $10^4\mathrm{E}_{51}^{0.22}\mathrm{n}_0^{-0.55}$years, see for example McCray (1987). After this time a momentum conserving phase starts in which the pressure decreases according to the adiabatic law. In order to avoid this stage which at the moment does not have a numerical counterpart, we limit ourselves to a lifetime of less than 3 10^4 years.

3. The asymmetric medium

In a medium with constant density an analytical solution is possible. We will now consider what happens if the medium is not symmetrical but presents an axial symmetry. The asymmetry can be characterised by defining the following radii: R_{up} is the radius at any given time of the expansion in the positive Z-direction, $\mathrm{R}_{\mathrm{down}}$ as the one in the negative Z direction, and R_{eq} as the radius of expansion in the X-Y plane, see Fig. 1. Is important to stress that the definitions of $\mathrm{R}_{\mathrm{down}}$, R_{up} and Z are always with respect to the Galactic plane so $\mathrm{R}_{\mathrm{down}}$ is always toward the plane (from either above or below) and R_{up} is always away.

3.1. The frames of reference

The frames of reference are defined as follows: A first frame X,Y,Z centered on the explosion and a second frame x,y,z where x-y is coincident with the galactic plane; in this second framework the center of the explosion has coordinates x_c, y_c and z_c.

3.2. Linear profile of the density

The following type of ISM is introduced:

$$\mathrm{n}(\mathrm{z}) = \mathrm{a}(1 - \frac{\mathrm{c}_\mathrm{a}|\mathrm{z}|}{\mathrm{b}}) \, , \tag{14}$$

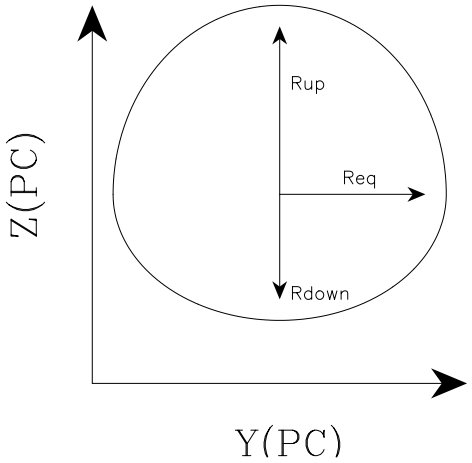

Fig. 1. Sketch of the asymmetric explosion projected on the Z-Y plane: R_{up}, R_{down} and R_{eq} are defined from a graphical point of view. The Cartesian axes are expressed in pc.

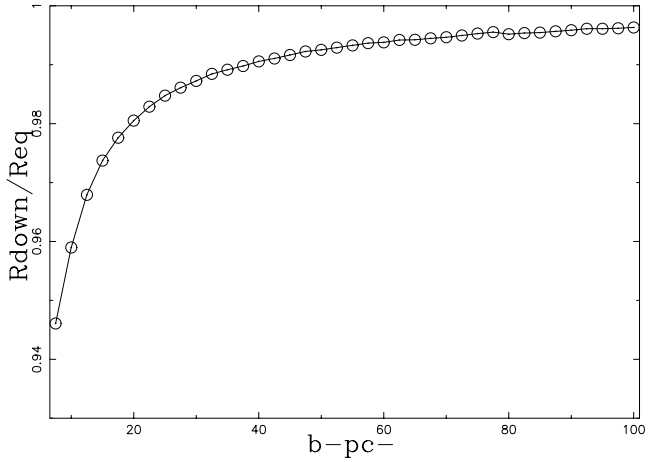

Fig. 2. The ratio R_{down}/R_{eq} versus b (in pc) when we have a linear decay of the density. The number of vertices along which we solve the differential equation is 2601, t_{final}=1.0 10^4 years, Δt = 1.0 10^{-3} 10^4years, a=0.15 particles cm^{-3} and c_a=0.1.

where a is the density at Z=0, b the strength of the gradient in pc and c_a is some constant fraction of a. Taking a=0.15 $\mathrm{particles\ cm^{-3}}$ there is a situation that resembles the ISM (Sect. 3.4) but with a linear decay of the density. The explosion is fixed in the galactic plane, z_c=0 pc, and is symmetrical with respect to the X-Y plane (R_{down} = R_{up}). The lifetime of the explosion, the only free parameter, is fixed at 10^4 years. The density is always decreasing away from the plane and R_{down} would always be greater than R_{eq} rather than less; in this case R_{down}=R_{up} because the explosion starts at z_c=0 (galactic plane). Therefore R_{down}/R_{eq} (always lower than one) versus b can be plotted in order to understand how the strength of the gradient changes the value of the asymmetry (Fig. 2).

3.3. An ISM with a Gaussian profile

An ISM is introduced with the following density profile

$$n(z) = n_G e^{-z^2/{H_G}^2}, \quad (15)$$

where n_G is the density at Z=0 and H_G the scale height in pc. The central value of the density is now fixed at n_G = 0.15 particles cm^{-3} and there is a situation similar to the first component of the ISM (Sect. 3.4). In Fig. 3 we have plotted the asymmetry R_{down}/R_{eq} versus H_G; also here this ratio is lower than one due to the fact that the sector in the z direction sweeps up less material than the x-y plane

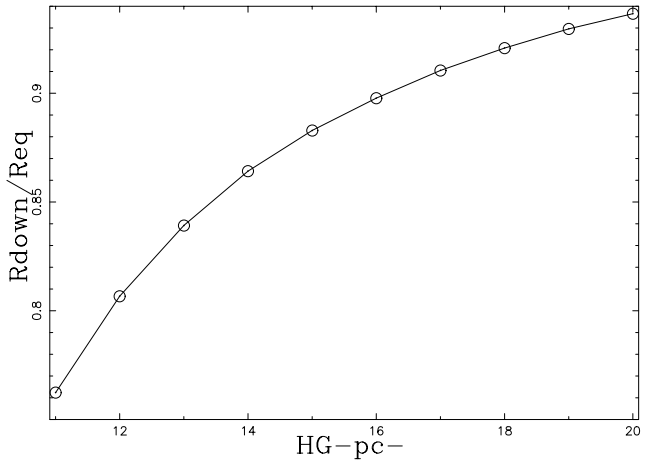

Fig. 3. The ratio R_{down}/R_{eq} is plotted versus H_G for an Gaussian decay of the density. Numerical input data as in Fig. 2

3.4. The standard ISM

The vertical density distribution of galactic HI is well-known; specifically it has the following three-component behaviour:

$$n(z) = n_1 e^{-z^2/{H_1}^2} + n_2 e^{-z^2/{H_2}^2} + n_3 e^{-|z|/H_3}. \quad (16)$$

Following Bisnovatyi-Kogan (1995) and Dickey & Lockman (1990) who extracted the data from Lockman (1984), we took n_1=0.395 $\mathrm{particles\,cm^{-3}}$, H_1=127 pc, n_2=0.107 $\mathrm{particles\,cm^{-3}}$, H_2=318 pc, n_3=0.064 $\mathrm{particles\,cm^{-3}}$, H_3=403 pc. This distribution of the galactic HI is valid in the range $0.4 \leq R \leq R_0$, where R_0 = 8.5 kpc and R is the distance from the center of the galaxy. In this case the expansion is in the ambient medium and the only free parameters are:

- The time t_{final} elapsed from the explosion which is set at 10^4 years.
- The distance from the galactic plane, which becomes the independent variable of the found asymmetries.

Mass accumulation stops when we reach the region where the sound speed exceeds the expansion velocity. This is because the thin layer approximation is no longer valid under such conditions. Theoretically speaking, two kind of asymmetries can be introduced: R_{down}/R_{eq} and R_{down}/R_{up} versus z_c, the distance of the explosion from the galactic plane, see Fig. 4 and Fig. 5

We find that:

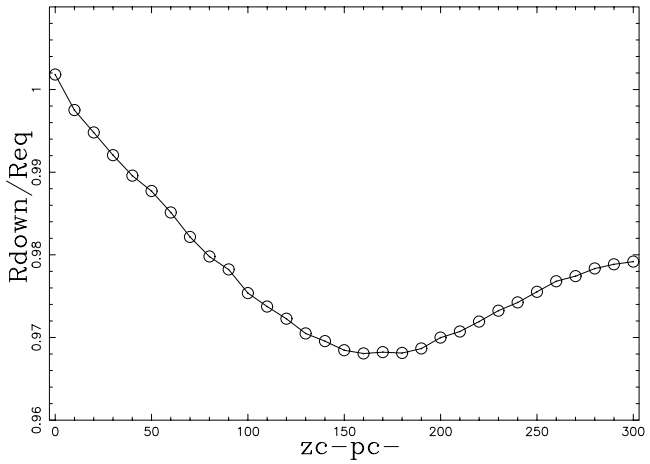

Fig. 4. $\mathrm{R_{down}/R_{mathrmeq}}$ versus $\mathrm{z_c}$ expressed in pc for a standard ISM. The number of faces is 2500, other numerical input as in Fig. 2

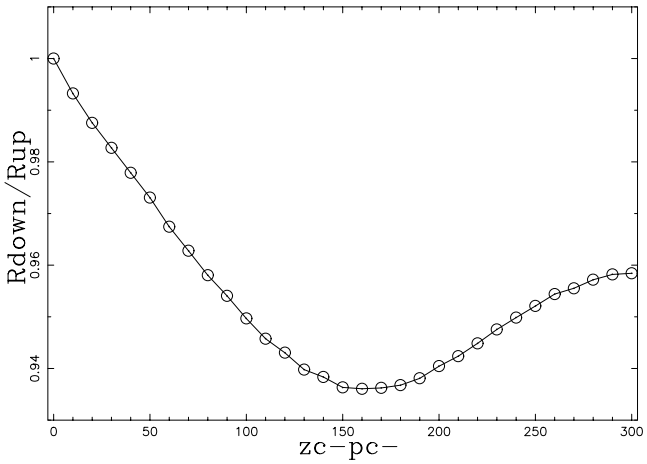

Fig. 5. $\mathrm{R_{down}/R_{up}}$ versus $\mathrm{z_c}$ expressed in pc for a standard ISM. Numerical input as in Fig. 2

– Given a certain value of $\mathrm{z_c}$ the inequality $\mathrm{R_{down}} < \mathrm{R_{eq}} < \mathrm{R_{up}}$ is always true. This could also be predicted from a theoretical point of view because in the z-direction the density diminishes progressively,
– In both cases there is a maximum asymmetry at ≈160 pc from the Galactic plane.

We can explain the asymmetries as follows:

– $\mathrm{R_{up}} > \mathrm{R_{eq}}$ because in the positive z direction ($\mathrm{z_c}$ fixed)the SNR sweeps up less material than in the x-y plane.
– $\mathrm{R_{up}} > \mathrm{R_{down}}$ because in the positive z direction ($\mathrm{z_c}$ fixed) the SNR sweeps up less material than in the negative z direction. We remember that we can cross z=0.
– $\mathrm{R_{eq}} > \mathrm{R_{down}}$ because in the x-y plane the SNR sweeps up less material than in the negative z direction.

The behaviour of $\mathrm{R_{eq}}$ versus the value of $\mathrm{z_c}$ is also reported: this numerical radius can be compared to the theoretical radius once the average density along the solid angle has been found numerically and inserted together with the corresponding height z in Eq. (11) (see Fig. 6). We remember that the remnant can cross z=0 across which the physical directions of up and down reverse.

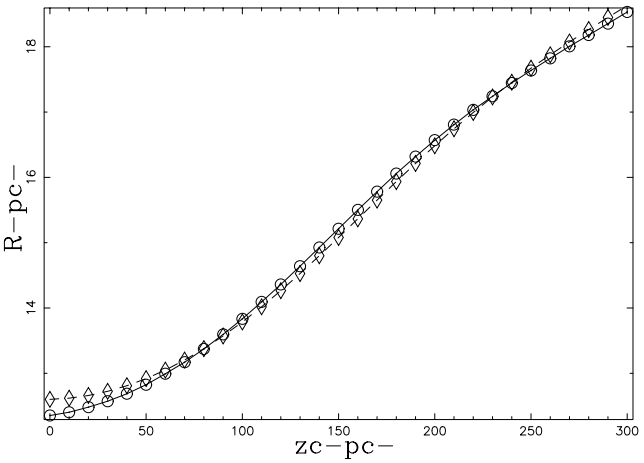

Fig. 6. The theoretical radius (dotted line+square) and the equatorial numerical radius $\mathrm{R_{eq}}$ (filled line + crosses) against $\mathrm{z_c}$ expressed in pc for a standard ISM. We have $\Delta \mathrm{t} = 5.0\ 10^{-4}\ 10^4 \mathrm{years}$ and the other numerical input are as in Fig. 2

3.5. The ring-shaped ISM

A local modification of the general formula for the ISM could be a ring shape with enhanced density in comparison to the classical value of Sect. 3.4.

A possible description is given by the following function:

$$\mathrm{n_R(R,Z)} = \mathrm{n_c} \exp \frac{-(\mathrm{R}-\mathrm{R_R})^2}{2\sigma_\mathrm{R}^2} \exp \frac{-\mathrm{Z}^2}{2\sigma_\mathrm{Z}^2}\,, \qquad (17)$$

the parameters adopted are:

R	$\sqrt{\mathrm{X}^2+\mathrm{Y}^2}$ the distance in the X-Y plane
$\mathrm{n_c}$	maximum central density
R	mean distance of the ring
σ_R	radial dependence of the density
σ_Z	Z dependence of the density

The density at any point of the galaxy will be the sum of the densities of the normal ISM and of the ring. This kind of medium allows the formation of an hour-glass shape.

3.6. Encounter with a denser cloud

The simplest model adopts an explosion in a medium with constant density $\mathrm{n_{medium}}$ which at a certain point of the expansion encounters a cloud (a semi-space delimited $\mathrm{Z} < \mathrm{Z_{cloud}}$) with greater density $\mathrm{n_{cloud}}$.

4. The SN models

A first check of our code can be done for an ISM with constant density, extracting the physical data from a historical Supernova. For this check, we used SN 1006. In this case, we know the elapsed time ($\mathrm{t_{final}}$) from the beginning of the explosion, as well as the observed value of the radius and the value of the ambient

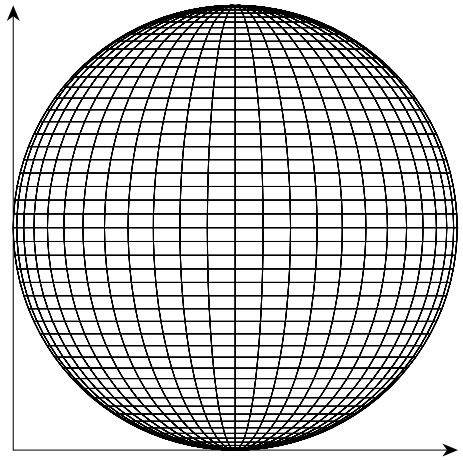

Fig. 7. The shape of the expanding envelope modelled by 2500 faces particularized for SN 1006. In this case the explosion is symmetrical because the density is constant; in particular n_0=0.1 $\frac{\text{particles}}{\text{cm}^3}$. t_{final}=0.974 10^4 years; for other numerical input see Fig. 2. We remember that X,Y and Z coordinates are given in pc. The two parameters that define the view point from the center of the 3D box are *lat–obs*=0 °, *long–obs*=0 °.

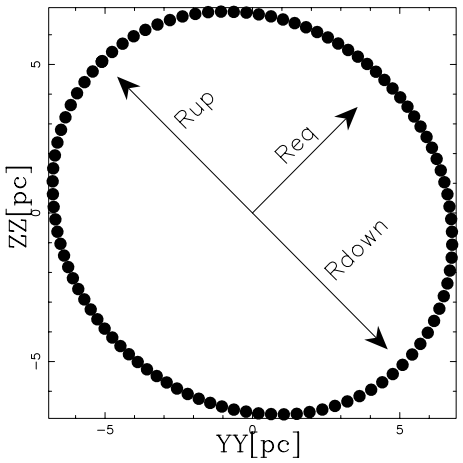

Fig. 8. Section of the explosion in the case of an Gaussian medium after a rotation of 45°along the X-axis; t_{final}=0.0974 10^4 years, n_G =0.15 particles /cm^3, H_G =7.0 pc, R_{eq}/R_{up}=0.88.

density. Therefore, the case of an explosion in a medium with a constant density (given from the observations) can be analysed and the percentage of reliability of our code can be introduced in an astrophysical context:

$$\epsilon = (1 - \frac{|(R_{obs} - R_{num})|}{R_{obs}}) \times 100 \quad , \tag{18}$$

R_{obs} is the observed radius and R_{num} the radius found through numerical analysis. If R_{num} = R_{obs} ϵ becomes 100 and if R_{num}=0 ϵ becomes 0. The test for SN1006 was made by inserting the astrophysical data extracted from Lang (1991) and Strom (1988); they are R_{obs}=6.35pc (the observed SN radius) and $n_0 = 0.1 \text{particles}/\text{cm}^3$ (the averaged value of the ISM density. The numerical results that are obtained inserting the averaged density, the SN lifetime (974 years, the time elapsed from the explosion to the astronomical measurement) gives a radius of 6.80pc (in the case of constant density the radius is equal in every direction); we obtain a value for ϵ (the percentage of reliability of our code) of 92.83%. It should be stressed that this good reliability is also given from the main adopted parameters: 10^{51}ergs, 10^4km/sec,. . . We remember that in the case of SN1006 we are already in the Sedov phase because using Eq. (9) and taking $n_0 = 0.1 \text{particles}/\text{cm}^3$, t $\approx$ $(420 \Leftrightarrow 840)$years is obtained which is less than the real lifetime of the SN (974years). The shape of the external envelope could be graphically presented by plotting the faces of the irregular polyhedron that represents the expansion layer,see for example Fig. 7, in which we have inserted the data of SN 1006. In order to take into account the great variety of perspectives, the parameters of the observer are introduced, which are the two angles of viewpoint from the center of a work-box in ° (*long-obs* angle in the X-Y plane) and *lat-obs* (vertical angle from the X-Y plane).

4.1. The Gaussian model

The model of SN 1006 can be refined by using the framework developed in Sect. 3.3. In effect, on referring to the radio-map of SN 1006 at 1370 MHz by Reynolds & Gilmore (1986), it can be observed that the radius is greatest in the north-east direction. Thus, by performing a rotation of $45°$, R_{up} of Fig. 1 can be identified with the radius in the north-east direction. From the radio-map previously mentioned we can extract the following observed radii R_{up}^{obs}= R_{down}^{obs}=6.8 pc and R_{up}^{obs}= 5.89 pc, where the apex stands for observed. From the previous data the observed asymmetry turns out to be $R_{eq}^{obs}/R_{up}^{obs} \approx 0.86$. In order to simulate this asymmetry we should first introduce three particularized percentage of reliability:

$$\epsilon_{up} = (1 - \frac{|(R_{up}^{obs} - R_{up}^{num})|}{R_{up}^{obs}}) \times 100 \quad , \tag{19}$$

where the index up stands for upward, the apex obs stands for observed and the index num stands for numerical,

$$\epsilon_{eq} = (1 - \frac{|(R_{eq}^{obs} - R_{eq}^{num})|}{R_{eq}^{obs}}) \times 100 \quad , \tag{20}$$

where the index eq stands for equatorial,

$$\epsilon_{asym} = (1 - \frac{|(R_{eq}/R_{up})^{obs} - (R_{eq}/R_{up})^{num})|}{(R_{eq}/R_{up})^{obs}}) \times 100, \tag{21}$$

where the index asym stands for asymmetry.

We model the asymmetrical shape of SN 1006 using Eq. 15 for the Gaussian density: in particular we inserted n_G = 0.15 $\text{particles}/\text{cm}^3$ (this value is a little bit greater that the averaged observed density, $0.1 \text{particles}/\text{cm}^3$) and H_G = 7pc. To visualise the results a section of the obtained ellipsoid is made in the YY-ZZ plane (see Fig. 8). The YY and ZZ axes are the transformation of Y and Z axes after a rotation of $45°$ along the X-axis. From the figure the elliptical shape of the simulation is clear thanks to which the observed asymmetry R_{eq}/R_{up} can be

Table 1. Expansion with decreasing H_G. The number of vertices along which we solve the differential equation is 441, the number of faces is 400, t_{final}=0.0974 10^4 years, $\Delta t = 1.0\ 10^{-4}\ 10^4$years, n_G =0.15 particles /cm^3.

H_G	R_{eq}/R_{up}
7.00	0.88
5.80	0.81
5.22	0.76
4.64	0.66
4.06	0.53
3.48	0.30
2.90	0.09

matched. The three percentages of reliability that characterize the whole shape are reported in Table 2. At the same time the possibility of obtaining a smaller value of the ratio R_{eq}/R_{up}, typical of the "barrel" SNR, can be explored. It should be remembered that in the case of SNR G296.5 the value $R_{eq}/R_{up} \approx 0.54$ can be reached (Gaensler 1998). To explore the possibility of obtaining greater values of asymmetry (smaller values of R_{eq}/R_{up}), several runs of our code in the Gaussian ISM case were made. In particular, the lifetime and central density that gave good values for SN 1006 were fixed and the scale height H_G was allowed to vary. The results are shown in Table 1 in which the increase of the asymmetry with the decrease of H_G is clear.

4.2. Comparison between different density gradients

The following questions can now be asked:

- Could the observed asymmetry of SN1006 be explained by a linear gradient or by the standard ISM?
- If the standard ISM is used, which coordinates of z_c should be used?

We can start from the last question by bootstrapping. In this case, after many iterations the value of $z_c \approx 200$ pc was found to produce the best results. Reported in Table 2 are the results of an expansion in a medium with a linear gradient, Gaussian and standard ISM. It is clear from the table that all three types of density gradient could produce a match with the averaged radius of SN1006 with a reliability that is greater than 90%. Conversely, a large asymmetry in the ratio R_{eq}/R_{up} could not be produced by the standard ISM but only by a linear or Gaussian density gradient.

4.3. The two-ring model

Using the framework developed in Sect. 3.5, a typical structure is presented in Fig. 9 in which *long–obs*=0 °and *lat–obs*=0 °(from this figure it is clear that a double-lobed flow can be produced starting from an initial spherical expansion); conversely, to show the rich morphology that the hour-glass shape could take on the

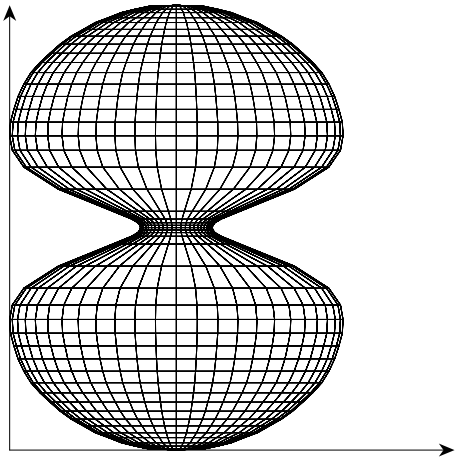

Fig. 9. The hour-glass (double-lobed flow) shape with *long–obs* =0°and *lat–obs*=0°. The parameters characterising the ring are σ_R=2.0 pc, σ_Z=0.2pc, n_c=100 particles/cm^3 and R_R=2.0pc. $\Delta t = 10.0\ 10^{-3}\ 10^4$years; for other numerical input see Fig. 2.

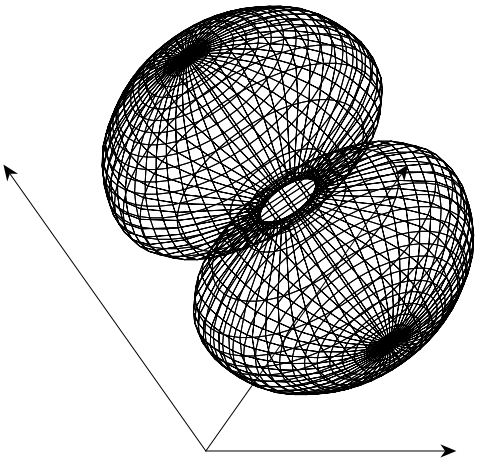

Fig. 10. The same as Fig. 9 but with *long–obs*=45 °and *lat–obs*= 45°

basis of the point of view of the observer, *lat–obs* = 10 °and *long–obs*=43°were introduced in order to produce Fig. 10.

To understand how it is possible to obtain a double-lobed flow, we made 3D ISO-density contours of the distribution of the interstellar medium. This surface is shown in Fig. 11 in which the chosen density was fixed at 80% of the central one. The shape of this 3D surface confirms that expansion is faster along the Z-direction (less mass swept-up), than along the equator (X-Y plane) (more swept-up mass). Another way to understand the change of the outline curvature is connected to the curvature change of the product of the two Gaussian distributions, see Eq. (17).

4.4. Two-density model

SNRs are also observed in the LMC and the radio shells are similar to those observed in the Milky Way. These shells present asymmetries in the direction of the associated HII regions, see Dickel & Milne (1998). Attention is concentrated on

Table 2. Expansion in different density gradients

type of medium	Parameters		$\epsilon_{\rm up}(\%)$	$\epsilon_{\rm eq}(\%)$	$\epsilon_{\rm asym}(\%)$
linear gradient	$a = 0.15 cm^{-3} ca = 0.2$ a	$b = 2.2$ pc	92.58	89.53	97.23
Gaussian gradient	$n_G = 0.15 cm^{-3}$	$H_G = 7.0$pc	94.9	92.5	97.74
standard ISM	$z_c = 200$pc		90.80	95.5	85.69

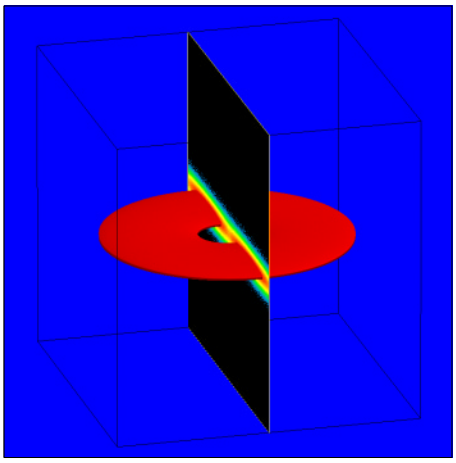

Fig. 11. Three dimensional surface of the ring density. The parameters characterising the ring are σ_R=2.0 pc, σ_Z=0.2pc, n_c=100 particles/cm^3 and R_R=2.0pc. The ISO-density contours are fixed at 80 particles/cm^3 and the three Eulerian angles characterising the point of view are 90,70 and 75. A 2-D coloured contour map of a slice that cross the center is also drawn. The *side* of the 3D-box is 8 pc

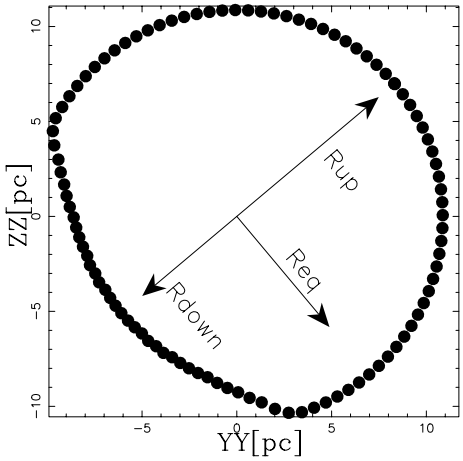

Fig. 12. Cross-cut of the explosion of N23:SNR(0506-680) after a rotation of -50°on the X axis. We start with an explosion with constant density n_{medium}=10 particles/cm^3 that a Z_{cloud}=-4.20pc encounters a cloud with density n_{cloud}=30 particles/cm^3 t_{final}=3.0 10^4 years and $\Delta t = 1.0\ 10^{-3}\ 10^4$years; for other numerical input see Fig. 2. The ratio R_{down}/R_{up} turns out to be 0.73.

N23:SNR(0506-680) and the physical parameters that can be extracted from the radio-observations are as follows:

$$\begin{array}{ll} R_{eq} & \approx 11.1 \text{ pc} \\ R_{up} & \approx 10.7 \text{ pc} \\ R_{down} & \approx 7.9 \text{ pc} \\ \text{ambient density} & \approx 10 \text{ particles /cm}^3 \end{array}$$

It is not known if a density gradient exists in the axial direction of the rotation plane of the LMC and, in order to fit the observations, the following parameters will be adopted in the simulation using the framework developed in Sect. 3.6:

$$\begin{array}{ll} n_{medium} & = 10 \text{ particles/cm}^3 \\ n_{cloud} & = 30 \text{ particles/cm}^3 \\ Z_{cloud} & = \text{-45 pc} \\ t_{final} & = 3.0\ 10^4 \text{ years} \end{array}$$

The result of the simulation is reported in Fig. 12 in which an additional rotation of -50°along the X axis was made. The meaning of the YY and ZZ axis of the figure is the same as in Sect. 4.1. In order to test the efficiency of this model we introduce two others particularized percentage of reliability:

$$\epsilon_{down} = (1 - \frac{|(R^{obs}_{down} - R^{num}_{down})|}{R^{obs}_{down}}) \times 100 \quad , \qquad (22)$$

Table 3. Efficiency in modelling N23

$\epsilon_{down}(\%)$	$\epsilon_{eq}(\%)$	$\epsilon_{up}(\%)$	$\epsilon_{asym-ud}(\%)$
99.47	97.89	98.44	98.99

where the index down is obvious, the apex obs stands for observed and the index num stands for numerical,

$$\epsilon_{asym-ud} = (1 - \frac{|(R_{down}/R_{up})^{obs} - (R_{down}/R_{up})^{num})|}{(R_{down}/R_{up})^{obs}}) \times 100\,, \qquad (23)$$

where the index asym-ud stands for up-down. The various efficiencies are reported in Table 3.

5. Conclusions

The shapes of SNRs present a rich morphology in which the departure from circular symmetry represents the norm rather than the exception. In order to simulate the great variety of shapes, the momentum conservation coupled with various type of ISM was used, and the following conclusions can be drawn:

– The presence of a weak density gradient that could be linear, Gaussian or ambient, produces weak departures from circular symmetry.

– A ring-shaped interstellar medium converts a symmetrical explosion into a double-lobed flow.

Acknowledgements. I thank the referee John R. Dickel and the Deputy Editor Jet Katgert for useful and detailed suggestions. The numerical code uses the subroutines extracted from "NUMERICAL RECIPES" for mathematical help. The plotting package is PGPLOT 5.2 developed by T.J.Pearson and we use PGXTAL developed by D.S. Sivia to trace the iso-surface.

References

Bisnovatyi-Kogan G.S., 1995, Review of Modern Physics 67, 661
Chevalier R.A., 1982, ApJ 258, 780
Dickel J.R., Eilek J.A., Jones E.M., 1992, ApJ 412, 648
Dickel J.R., Milne D.K., 1998, ApJ 115, 1057
Dickey J., Lockman F., 1990, ARA&A 28, 215
Gaensler B.M., 1998, ApJ 493, 781
Lang K.R., 1991, Astrophysical Data. Planets and Stars. p. 705
Lockman F.J., 1984, ApJ 293, 90
McCray R., 1987, In: Dalgarno A., Layzer D. (eds.) Spectroscopy of Astrophysical Plasmas. Cambridge University Press, Cambridge, p. 271
Press W.H., Teukolsky,S.A., Vetterling W.T., Flannery B.P., 1992, Numerical Recipes in Fortran. Cambridge University Press, Cambridge, p. 706
Reynolds S.P., Gilmore D.M., 1986
Strom R.G., 1988, MNRAS 230, 231